JOC The Journal of Organic Chemistry

ARTICLE

pubs.acs.org/joc

Transition States and Energetics of Nucleophilic Additions of Thiols to Substituted α,β-Unsaturated Ketones: Substituent Effects Involve Enone Stabilization, Product Branching, and Solvation

Elizabeth H. Krenske,*[,†,§] Russell C. Petter,[‡] Zhendong Zhu,[‡] and K. N. Houk*[,§]

[†]School of Chemistry, University of Melbourne, and Australian Research Council Centre of Excellence for Free Radical Chemistry and Biotechnology, VIC 3010, Australia

[§]Department of Chemistry and Biochemistry, University of California, Los Angeles, California 90095, United States

[‡]Avila Therapeutics, 100 Beaver Street, Waltham, Massachusetts 02453, United States

S Supporting Information

ABSTRACT: CBS-QB3 enthalpies of reaction have been computed for the conjugate additions of MeSH to six α,β-unsaturated ketones. Compared with addition to methyl vinyl ketone, the reaction becomes 1−3 kcal mol^{-1} less exothermic when an α-Me, β-Me, or β-Ph substituent is present on the C=C bond. The lower exothermicity for the substituted enones occurs because the substituted reactant is stabilized more by hyperconjugation or conjugation than the product is stabilized by branching. Substituent effects on the activation energies for the rate-determining step of the thiol addition (reaction of the enone with MeS$^-$) were also computed. Loss of reactant stabilization, and not steric hindrance, is the main factor responsible for controlling the relative activation energies in the gas phase. The substituent effects are further magnified in solution; in water (simulated by CPCM calculations), the addition of MeS$^-$ to an enone is disfavored by 2−6 kcal mol^{-1} when one or two methyl groups are present on the C=C bond ($\Delta\Delta G^{\ddagger}$). The use of CBS-QB3 gas-phase energies in conjunction with CPCM solvation corrections provides kinetic data in good agreement with experimental substituent effects. When the energetics of the thiol additions were calculated with several popular density functional theory and ab initio methods (B3LYP, MPW1PW91, B1B95, PBE0, B2PLYP, and MP2), some substantial inaccuracies were noted. However, M06-2X (with a large basis set), B2PLYP-D, and SCS-MP2 gave results within 1 kcal mol^{-1} of the CBS-QB3 benchmark values.

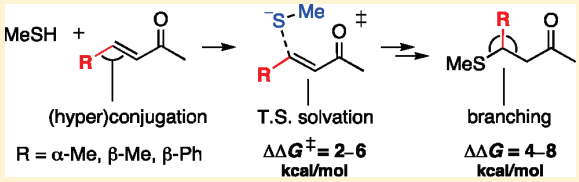

INTRODUCTION

The discovery of Michael acceptors that bind covalently to specific enzyme thiol groups is an important current target in drug design. Michael additions involving biological thiols are also toxicologically important, and many Michael acceptors have been studied in assessments of quantitative structure−activity relationships. However, the factors that determine how the rate of addition depends on the substituents on the Michael acceptor are not well established. We present here a computational evaluation, providing quantitative data about effects of substituents on reactant and product stabilities, transition state energies, and how these are influenced by solvation. We also benchmark the performance of common computational methods for predicting the energetics of thiol additions. Some significant errors in predictions of thermodynamics by frequently used methods are identified.

Here we investigate the base-catalyzed conjugate addition of thiols to α,β-unsaturated ketones, as shown in Scheme 1.[1] Targeting these reactions to therapeutically relevant enzyme thiol groups has led to the development of inhibitors of cysteine-dependent enzymes such as cysteine proteases,[2] and analogous alcohol additions have been explored in the development of irreversible proteasome inhibitors.[2c,d] More recently, Michael acceptors have been employed as bond-forming functional groups in selective irreversible kinase inhibitors.[3] Notable examples include the ErbB kinase inhibitors neratinib (HKI-272), in phase III trials for the treatment of breast cancer,[4] and Tovok (BIBW-2992), in phase III trials for the treatment of lung cancer.[5] In addition, PCI-32765 (Phase I) is an irreversible inhibitor of Bruton's tyrosine kinase (Btk), which plays a key role in B cell activation and proliferation (Chart 1).[6]

Scheme 1

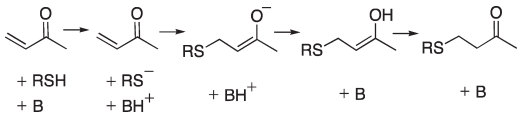

Received: April 12, 2011
Published: May 16, 2011

 © 2011 American Chemical Society

BeiGene Exhibit 1157.001
BeiGene v. Pharmacyclics
PGR2024-00009

Chart 1

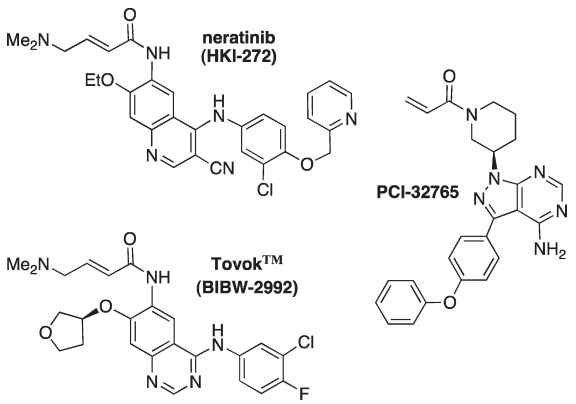

Scheme 2. Rate and Equilibrium Constants Reported for (a) Additions of Glutathione[9c] and (b) Additions of PhSH to α,β-Unsaturated Ketones[10]

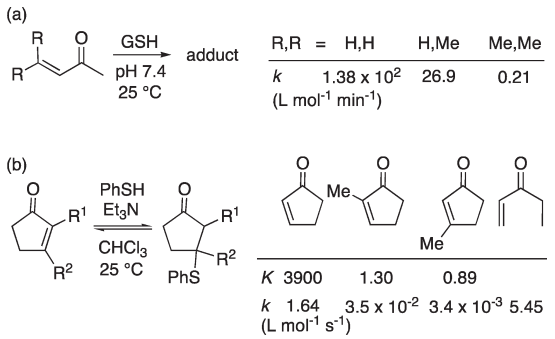

The emerging importance of Michael acceptors as key pharmacophores in the design of irreversible inhibitors of clinically important protein targets motivates a deeper understanding of the factors that modulate their reactions with biologically important nucleophiles. Numerous studies have investigated the influence of the thiol R group on reactivity toward conjugate addition.[7] Here we examine the effects of substituents on the Michael acceptor. In general, conjugate additions to Michael acceptors are hampered by alkyl substituents at the α or β position of the C=C bond and by Ph substituents at the β (but not α) position.[8] Rate data reported[9] for acyclic enones and other Michael acceptors indicate that β-Me substitution reduces the rate of addition less than α-Me, β,β-dimethyl, or β-Ph substitution, and that in some cases the overall reactivity of the enone is reduced because the addition is reversible. Rate constants reported for the additions of glutathione to enones at pH 7.4 are shown in Scheme 2a.[9c] Rate and equilibrium constants have also been reported for Et_3N-catalyzed additions of PhSH to cyclic α,β-unsaturated ketones in chloroform, and are shown in Scheme 2b.[10]

Several groups have devised schemes for predicting the reactivities of Michael acceptors toward thiols on the basis of calculated ground-state properties.[11] Kinetic data have been correlated with properties such as atomic charges, electrophilicities, steric parameters, and the reaction energies for thiol adduct formation.[9c,d,11]

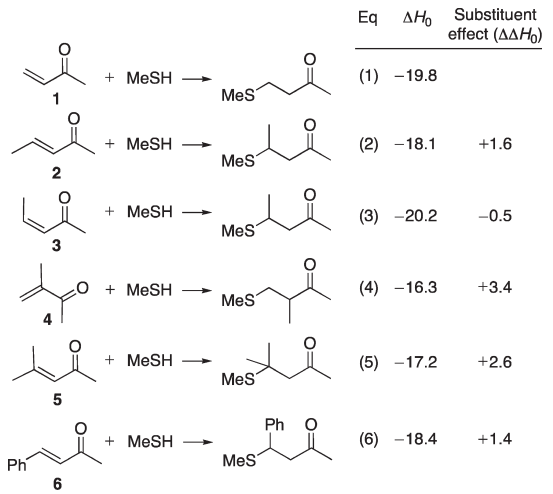

Figure 1. Enthalpies of addition of MeSH to the α,β-unsaturated ketones **1**−**6** (CBS-QB3, kcal mol^{-1}). Substituent effect is the difference from eq 1.

Schüürmann et al. have devised schemes for predicting the rates of additions of glutathione to Michael acceptors based on calculated local electrophilicity parameters.[9c,d,11e] Very recently, Cronin et al.[12] reported B3LYP calculations on the additions of methanethiol and cysteine to 22 Michael acceptors. The mechanism that they considered entailed a concerted four-center addition of the neutral thiol across the C=C bond. Here we report calculations on the additions of thiols to α,β-unsaturated ketones, in which the rate-determining step is the addition of the MeS^- anion to the enone to generate an intermediate enolate. We use high-accuracy CBS-QB3 calculations[13] to obtain quantitative kinetic and thermodynamic data describing the effects of enone substitution and the influence of solvation. Reaction energies are computed for the transformation of six α,β-unsaturated ketones into their β-methylthio adducts. CBS-QB3 data are then used in conjunction with a continuum solvent model to evaluate substituent effects on the rate-determining thiolate addition step in water. The kinetics are shown to be controlled not by steric effects, but by reactant stabilization. The calculations provide information about transition-state geometries that is of relevance to drug design.

In recent studies of related C−C and C−O bond-forming reactions (aldol, Mannich, α-aminoxylation, and Diels−Alder reactions), substantial errors were found in the reaction enthalpies and substituent effects computed with commonly used density functional theory methods.[14,15] Similar features are found here for the C−S bond-forming reactions. Several well-established functionals perform with low accuracy, but the newer methods M06-2X, B2PLYP-D, and SCS-MP2 are found to yield good agreement with CBS-QB3.

THEORETICAL CALCULATIONS

CBS-QB3 calculations[13] gave enthalpies for the addition of MeSH to the α,β-unsaturated ketones **1**−**6** (Figure 1). Activation energies and reaction energies for the addition of MeS^- to **1**−**6** were also calculated with CBS-QB3. Experimental measurements for these thermodynamic and kinetic quantities have not been reported. However, the CBS-QB3 method has been shown[13] to provide high-accuracy thermochemical data (MAD for the G2/97

BeiGene Exhibit 1157.002
BeiGene v. Pharmacyclics
PGR2024-00009

test set 1.10 kcal mol^{-1}, compared with 0.94 kcal mol^{-1} for the G3 composite method[16]) and is also expected to provide reliable energies of activation. For comparison, previous benchmarking of CBS-QB3 against the experimental activation enthalpies for nine pericyclic reactions yielded an MAD of 2.3 kcal mol^{-1}.[17] It provided MADs of 0.6−2.5 kcal mol^{-1} when benchmarked against databases of barrier heights for hydrogen transfer, heavy atom transfer, nucleophilic substitution, and unimolecular and association reactions compiled by Truhlar from experimental and high-level quantum chemical data.[18]

The performance of several common density functional theory methods (the hybrid GGAs B3LYP,[19] MPW1PW91,[20] B1B95,[21] PBE1PBE (PBE0),[22] the hybrid meta-GGA M06-2X,[23] the double hybrid B2PLYP,[24] and its dispersion-corrected variation B2PLYP-D[25]), of second-order Møller−Plesset perturbation theory (MP2),[26] and of the spin-component scaled variant SCS-MP2,[27,28] was assessed with respect to the CBS-QB3 benchmarks. Optimizations with these methods used the 6-31+G(d) basis set. Single-point energies were also calculated with the 6-311G(2d,p) basis. The DFT and MP2 zero-point energies were calculated from the 6-31+G(d) vibrational frequencies without scaling. Enthalpies are quoted at 0 K.

Each reactant and product was subjected to conformational searching at the B3LYP/CBSB7 level in order to identify the lowest-energy isomer. The α,β-unsaturated ketones **1**, **2**, **3**, **5**, and **6** were found to be more stable in the s-*cis* conformation, while **4** was more stable in the s-*trans* conformation. Experimental and computational studies of these species' conformational equilibria have been reported previously.[29]

Free energy surfaces for the reactions in solution were obtained by calculating CPCM[30] free energies of solvation in water (ε = 78.39) at the B3LYP/6-31+G(d) level (UAKS radii) and adding these values to the CBS-QB3 gas-phase free energies. This methodology has previously been used to provide accurate estimations of substituent and solvation effects in S_N2 reactions.[31]

Transition state optimizations were conducted for additions of MeS^- to both the s-*cis* and the s-*trans* conformer of each enone. In the gas phase (B3LYP/CBSB7), only transition states involving the s-*cis* enones could be located. However, when optimizations were conducted in solution [CPCM, B3LYP/6-31+G(d)], both s-*cis* and s-*trans* TSs could be found. The s-*cis* TS arrangement remained the most stable for all enones except **4**.

The nature of stationary points was checked by means of frequency calculations, and transition states were further verified by IRC calculations.[32] All calculations were performed using the Gaussian 03 software package,[33] except for the M06-2X and B2PLYP(-D) calculations, which were performed in Gaussian 09.[34] Optimizations and single-point energy calculations were performed using the default SCF convergence settings and fine integration grid. To test for grid effects, single-point energies were also calculated using the UltraFine grid with SCF=Tight. The resulting energies varied by no more than 0.2 kcal mol^{-1} from those reported here. CPCM solvation energies were subjected to similar checks, and found to vary by no more than 0.02 kcal mol^{-1}. Molecular structures were drawn with the CYLview program.[35]

RESULTS AND DISCUSSION

Thermodynamics of Thiol Additions. CBS-QB3 reaction enthalpies for the addition of MeSH to the α,β-unsaturated ketones **1**−**6** (eqs 1−6) are presented in Figure 1. The absolute values of ΔH_0 are shown, along with the changes in ΔH_0 caused by substituents on the C=C bond.

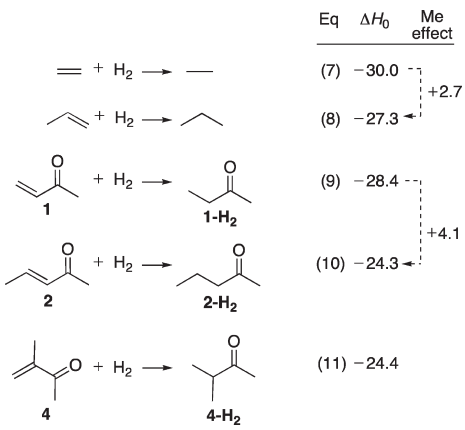

Figure 2. Enthalpies of hydrogenation of unsaturated molecules (CBS-QB3, kcal mol^{-1}).

The additions of MeSH to **1**−**6** are calculated to be exothermic by 16−20 kcal mol^{-1} in the gas phase. The reaction of the parent enone (**1**) has an enthalpy of −19.8 kcal mol^{-1}. All of the substituted derivatives react less exothermically than **1**, except for **3**. The reaction of **3** is 0.5 kcal mol^{-1} more exothermic than reaction of **1**, due to the relief of the steric crowding between the two *cis* substituents on the C=C bond. The *trans* isomer (**2**), where such steric effects are absent, reacts 1.6 kcal mol^{-1} less exothermically than the parent enone. A second β-Me group (**5**) lowers the exothermicity by a further 1.0 kcal mol^{-1} (approximately equal to the sum of *cis* and *trans* β-Me effects). A methyl group at the α position (**4**) reduces the exothermicity by 3.4 kcal mol^{-1}, while a phenyl group at the β position (**6**) reduces the exothermicity by 1.4 kcal mol^{-1}. The β-Ph effect is approximately the same as the β-Me effect.

Ignoring longer-range intramolecular interactions, the calculated methyl effects are the net result of two opposing contributions: (i) stabilization of the reactant by hyperconjugation between Me and the C=C−C=O group, and (ii) stabilization of the product due to branching. The positive values of $\Delta\Delta H_0$ (except for **3**) indicate that reactant stabilization by the substituent outweighs product stabilization.

A measure of the hyperconjugative stabilization of an enone by a β-methyl group is provided by the hydrogenation reactions 7−10 in Figure 2. These reactions assess hyperconjugation without complications from branching effects involving the SMe group. Hyperconjugation stabilizes the enone **2** more strongly than an isolated alkene: the hydrogenation of **2** is 4.1 kcal mol^{-1} less exothermic than that of **1** whereas hydrogenation of propene is only 2.7 kcal mol^{-1} less exothermic than that of ethene. An α-Me group has an almost identical effect on the hydrogenation enthalpy as a β-Me group (**4**, eq 11). The hydrogenations are isoenergetic because **4** and **4-H$_2$** are, respectively, stabilized over their isomers **2** and **2-H$_2$** by almost the same amounts; the former (**4**) due to the 1,1-disubstituted double bond and the latter (**4-H$_2$**) due to the higher degree of branching.[36]

Methyl effects on the MeSH additions are smaller than those on the hydrogenations. Here, additional branching interactions involving the SMe group in the product provide further compensation for the loss of hyperconjugative stabilization from the

BeiGene Exhibit 1157.003
BeiGene v. Pharmacyclics
PGR2024-00009

Scheme 3

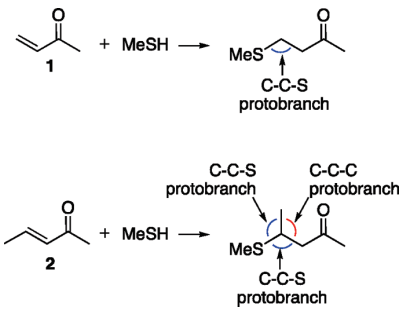

enone. The additional protobranches[37] gained in the MeSH additions are illustrated in Scheme 3. Addition of MeSH to **2** generates two more protobranches than addition to **1**. Thus, the reaction of MeSH with **2** is only 1.6 kcal mol^{-1} less exothermic than reaction with **1**, compared with 4.1 kcal mol^{-1} for the hydrogenations. A second β-Me group (**5**) leads to a further three new protobranches, and a further 1.0 kcal mol^{-1} loss of exothermicity.

Although the hydrogenations of the β- and α-Me derivatives **2** and **4** are almost isoenergetic (eqs 10 and 11), the addition of MeSH to **4** is 1.8 kcal mol^{-1} less exothermic than addition to **2**. Addition of MeSH introduces two new protobranches into **2-H$_2$** but only one new protobranch into **4-H$_2$**; some additional exothermicity is therefore recovered in the reaction of **2**.

Performance of Density Functional Theory and ab Initio Methods for the Thermodynamics of Thiol Additions. Enthalpies for reactions 1 and 5 were calculated with a range of commonly used density functional theory and ab initio methods, in order to assess the accuracy of the predicted energetics. Comparisons between the calculated enthalpies and the CBS-QB3 benchmark values are given in Table 1. Most of the DFT methods, when used in conjunction with the 6-31+G(d) basis set, yield poor agreement with CBS-QB3. The absolute deviations range from 0.8 to 10.3 kcal mol^{-1} in all but one case, and the methyl substituent effect is predicted to be 0.9−6.6 kcal mol^{-1} larger than the benchmark value of 2.6 kcal mol^{-1}. The best performing hybrid functionals (averaging over the two reactions) are MPW1PW91 and PBE1PBE, but even these functionals yield absolute errors well outside chemical accuracy. The double hybrid B2PLYP also does not provide chemical accuracy, but its dispersion-corrected variant (B2PLYP-D) yields energies within 1 kcal mol^{-1} of CBS-QB3 for both reactions.

Calculation of single-point energies with the 6-311G(2d,p) basis set (in conjunction with the 6-31+G(d) zero-point energies) led to no improvement in accuracy for most functionals, except for M06-2X, which gave enthalpies within 0.2 kcal mol^{-1} of the CBS-QB3 values with the larger basis set (see Table 1 and Supporting Information).

MP2 theory provides a relatively accurate estimation of the methyl effect (2.1 kcal mol^{-1}), but it overestimates the reaction exothermicities by 3−4 kcal mol^{-1}. The spin-component scaled SCS-MP2 variant is much more accurate, yielding absolute enthalpies within 1 kcal mol^{-1} of CBS-QB3.

Except for M06-2X and B2PLYP-D, the density functional methods underestimate the reaction exothermicity for the more highly substituted enone. Branching-related errors like these have been reported previously, and traced by Grimme to deficiencies in the functionals' treatment of medium-range correlation.[36]

Table 1. Performance of Various Density Functional Theory and ab Initio Methods for the Reaction Enthalpies of Eqs 1 and 5[a]

	equation 1		equation 5		
method	ΔH_0	error[b]	ΔH_0	error[b]	Me effect
CBS-QB3	−19.8		−17.2		2.6
B3LYP	−16.1	3.7	−6.9	10.3	9.2
MPW1PW91	−22.0	−2.3	−13.4	3.8	8.7
B1B95	−19.8	0.0	−12.2	5.0	7.6
PBE1PBE	−23.6	−3.8	−15.4	1.8	8.2
M06-2X	−22.3	−2.6	−18.9	−1.7	3.5
M06-2X/6-311G(2d,p)[c]	−19.8	0.0	−17.0	0.2	2.8
B2PLYP	−18.8	0.9	−12.4	4.8	6.4
B2PLYP-D	−20.7	−0.9	−16.4	0.8	4.3
MP2	−23.1	−3.3	−21.0	−3.8	2.1
SCS-MP2	−20.7	−0.9	−17.9	−0.7	2.8

[a] The 6-31+G(d) basis set was used for all calculations except where specified. Enthalpies are in kcal mol^{-1}. [b] Difference from CBS-QB3. [c] Electronic energy calculated with the 6-311G(2d,p) basis set at the 6-31+G(d) geometry and used in conjunction with the 6-31+G(d) zero-point energy.

Kinetics of Thiolate Additions. The rate-determining step in the base-catalyzed conjugate addition of a thiol is the reaction of the thiolate (or its ion pair with a protonated organic base, Scheme 1) with the α,β-unsaturated ketone to generate the enolate.[7a−d] In Cronin's[12] recent DFT study, these reactions were modeled by transition states entailing concerted addition of the thiol across the C=C bond of the Michael acceptor. The activation energies for this process were, however, in the range of 52−59 kcal mol^{-1}, and a stepwise process involving an enolate intermediate is much more likely. Rozas et al.[38] previously used semiempirical calculations to study conjugate additions of several biologically relevant thiolates. They found that in the gas phase, a complex of the reactants precedes the transition state for C−S bond formation. The complex and the TS were both lower in energy than the reactants. We have performed CBS-QB3 calculations on the additions of MeS$^-$ to **1**−**6**. These too proceed via a reactant complex in the gas phase. The geometries of the transition states are shown in Figure 3.

Two distinct transition-state geometries are found in the gas phase. The enone is s-*cis* in all of the transition states, but the MeS$^-$ ion can add to the C=C bond in either a *syn* or an *anti* conformation. For enones **1** and **2**, only *anti* TSs were found in the gas phase (**TS-1** and **TS-2**, Me−S···C=C dihedral 171° and 166°, respectively). For the other four enones, both *syn* and *anti* TSs were located, and the *syn* isomer (dihedral angle 14−28°) was lower in energy (**TS-3**−**TS-6**). The *syn* arrangement places the sulfur lone pairs further from the electron density of the C=C bond, and also enables an attractive electrostatic interaction between the MeS$^-$ hydrogens and the carbonyl oxygen. The *syn* geometry is the most stable conformation for all six of the enolates.

Both *syn* and *anti* transition states could be located by optimization in water [CPCM, B3LYP/6-31+G(d)]. The *syn* arrangement was usually still preferred, but variations were evident in the Me−S···C=C dihedral angle that indicated that the attractive interaction between the MeS$^-$ hydrogens and the

BeiGene Exhibit 1157.004
BeiGene v. Pharmacyclics
PGR2024-00009

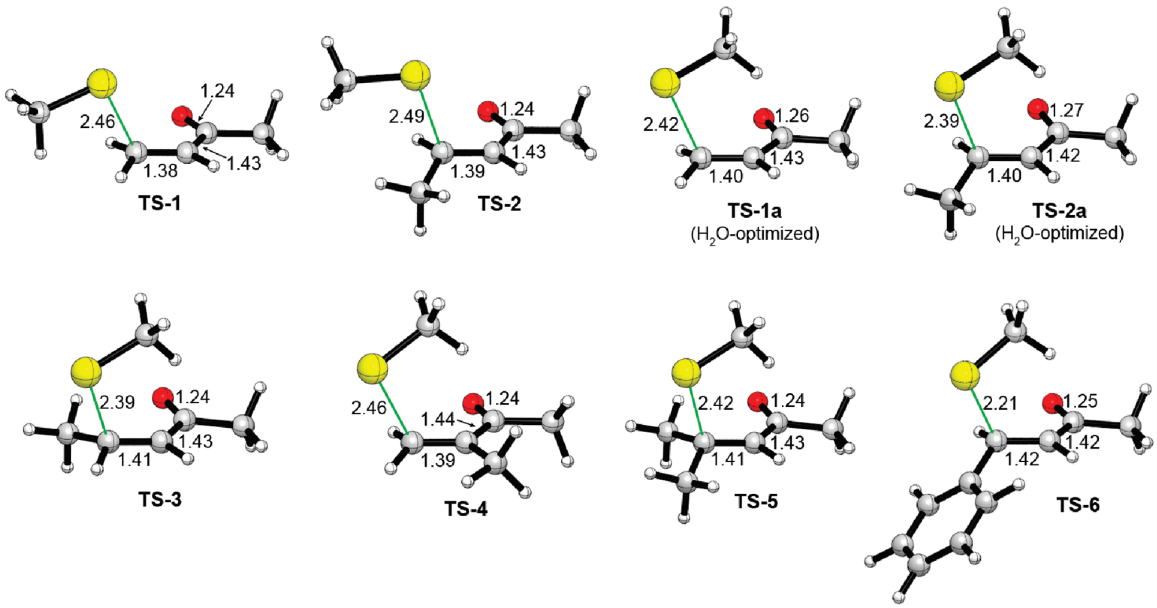

Figure 3. Transition structures for addition of MeS^- to the α,β-unsaturated ketones **1**−**6**. Transition states were optimized in the gas phase at the B3LYP/CBSB7 level, except for **TS-1a** and **TS-2a**, which were optimized in CPCM water at the B3LYP/6-31+G(d) level. Bond distances are in Å.

carbonyl oxygen is of less importance in solution. The S···C bond was 0.04−0.13 Å shorter in the solution-optimized analogues of **TS-3**−**TS-5**, but the bond lengths in the enone fragment varied only by 0.01−0.03 Å from the gas-phase values. Because *syn* transition states could not be located in the gas phase for enones **1** and **2**, we have taken the solution-optimized *syn* TSs for these enones as approximations for the true *syn* transition states. They are depicted in Figure 3 as **TS-1a** and **TS-2a**, respectively. CBS-QB3 single-point calculations indicate these structures to be 2−3 kcal mol^{-1} lower in energy than the *anti* transition states, **TS-1** and **TS-2** ($\Delta\Delta G^{\ddagger}$).

Steric clashing between the nucleophile and the enone is of only minor importance in the thiolate additions. In the gas-phase structures whose conformations allow a direct comparison (**TS-1** vs **TS-2**, and **TS-3** vs **TS-5**), the S···C distance becomes 0.03 Å longer with each successive methyl substitution. This is a small effect; by contrast, in the S_N2 reactions of Cl^- with R−Cl, the average Cl···C distance increases from 2.44 to 2.54 and 2.84 Å on going from R = Et to ^{i}Pr to ^{t}Bu.[39]

Free energy profiles were calculated for the additions of MeS^- to **1**−**6** in the gas phase and in water. These are shown in Figure 4. The solution-optimized *syn* TSs for **1** and **2** (**TS-1a** and **TS-2a**) are used for the analysis, although the higher-energy *anti* TSs (**TS-1** and **TS-2**) are also included as dashed lines.

In the gas phase, the formation of the enolates is exergonic by 2.6−7.1 kcal mol^{-1}, and has a low barrier (−4.1 to 3.3 kcal mol^{-1} relative to reactants). The *cis* enone **3** and the Ph-substituted enone **6** react more exergonically than **1**, while the other substituted enones react less exergonically. There is no clear correspondence between the activation energies and the energetics. In particular, the enones **5** and **6** have much lower activation energies than would be predicted from the values of ΔG.

When solvation is taken into account, the free-energy profiles fall into agreement with known substituent effects.[9,10] The values of ΔG for MeS^- addition in water vary from 12.9 to 21.6 kcal mol^{-1} and the values of $\Delta G^{\ddagger}$ range from 19.0 to 24.8 kcal mol^{-1}. The parent enone has the lowest value of ΔG, and the lowest barrier. The values of ΔG for the monomethyl-substituted enones **2**−**4** are 1.0−4.6 kcal mol^{-1} higher, and that of the dimethyl-substituted enone **5** is 8.7 kcal mol^{-1} higher than **1**. The activation energy increases by 3.1−4.1 kcal mol^{-1} when a single methyl group is present (**2**−**4**), while dimethyl substitution (**5**) raises the barrier by 5.8 kcal mol^{-1}.

The calculated methyl effects in water mirror those reported for additions of glutathione to enones, acroleins, and acrylates.[9] These additions are reported to be impeded substantially by α-Me and β,β-dimethyl substitution, and to a smaller degree by a β-Me group. The barriers also reflect qualitatively the rates measured for additions of PhSH to α-Me and β-Me cyclopentenones (Scheme 1),[10] although the extra β-alkyl group in cyclopentenones means the comparison is not a direct one.

Substituent effects on the formation of the enolates include contributions from the same intramolecular interactions discussed above for the overall addition of MeSH (Figure 1). For the methyl-substituted enones **2**, **4**, and **5**, the extra branching in the enolates (and the transition structures leading to them) is not sufficient to counterbalance the loss of hyperconjugative stabilization from the enones. Solvation also plays a crucial role. In water, reactions of the Me-substituted enones become even less favorable relative to the parent than they are in the gas phase. The values of $\Delta\Delta G$(substituted−unsubstituted) are 1.1−5.5 kcal mol^{-1} more positive in solution, while values of $\Delta\Delta G^{\ddagger}$ are 2.2−6.7 kcal mol^{-1} more positive. The solvation energies of the enones and transition states, and the contributions of solvation to the total activation energies and reaction energies are listed in Table 2. The contribution of solvation to the activation energy ($\Delta G_{solv}^{\ddagger}$) becomes increasingly less favorable on going from the parent to more highly substituted derivatives. This is largely due to more diffuse distribution of negative charge in the larger

BeiGene Exhibit 1157.005
BeiGene v. Pharmacyclics
PGR2024-00009

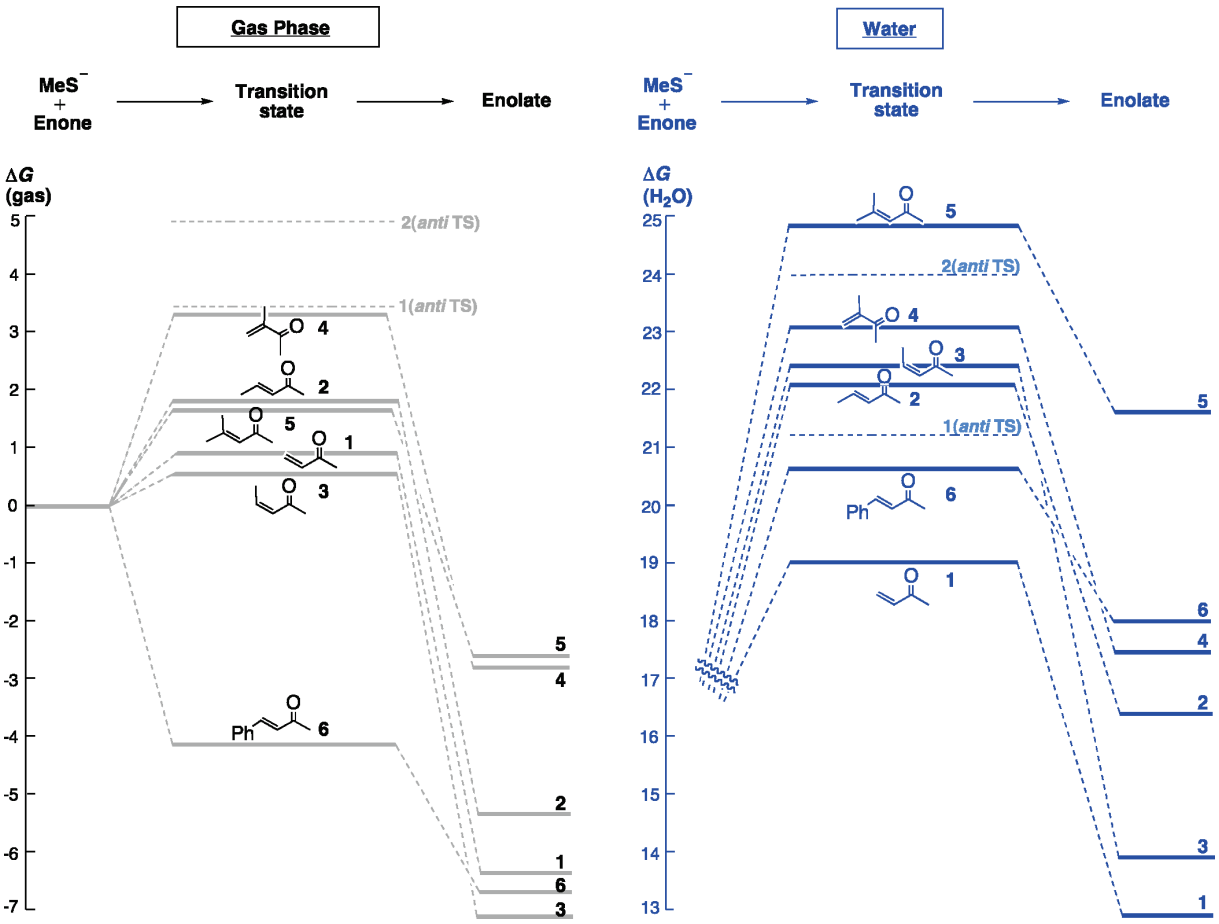

Figure 4. Free energy surfaces for addition of MeS^- to **1**−**6** in the gas phase (black) and water (blue). Gas-phase free energies were calculated with CBS-QB3, and solution-phase data were obtained by correcting the CBS-QB3 values with CPCM free energies of solvation at the B3LYP/6-31+G(d) level. Each plot is labeled with the structure of the enone. Free energies are in kcal mol^{-1} at 1 mol L^{-1} and 298.15 K. Reactant complexes are not shown.

Table 2. CPCM Solvation Energies of Enones and Transition States, and Contributions of Solvation to the Total Activation Energy and Reaction Energy in Water[a]

enone	G_{solv}(Enone)	G_{solv}(TS)	$\Delta G_{solv}^{\ddagger}$	ΔG_{solv}
1	−3.0	−53.6[b]	17.8	19.2
2	−4.2	−52.6[c]	19.1	21.7
3	−3.5	−50.3	21.8	21.0
4	−2.4	−51.3	19.8	20.3
5	−3.4	−48.9	23.1	24.2
6	−4.5	−48.3	24.8	24.7

[a] B3LYP/6-31+G(d), kcal mol^{-1}, 1 mol L^{-1}, 298.15 K. [b] **TS-1a**. [c] **TS-2a**.

transition states. The solvation energies of the enones also contribute to the ordering of some barriers.

The most pronounced solvent effect is seen with the Ph-substituted enone **6**. In the gas phase, addition of MeS^- to **6** is 5.0 kcal mol^{-1} more favorable than addition to **1** ($\Delta\Delta G^{\ddagger}$), but in water it is 1.7 kcal mol^{-1} less favorable. The low gas-phase barrier reflects the lower energy of the LUMO of **6**.[40] In solution, this barrier-lowering effect is lost because of the large solvation penalty. $\Delta G_{solv}^{\ddagger}$ for **TS-6** is 7 kcal mol^{-1} higher than for **TS-1**.

Michael additions are often reversible.[8] Consistent with this, the overall transformation of **1**−**6** to their MeSH adducts in water is calculated to have values of ΔG ranging from −1.9 to −10.0 kcal mol^{-1} (see Supporting Information). The free energies for the overall transformation follow the same order as those for the rate-determining addition of MeS^- (Figure 3). Relatively low barriers for the reverse of the rate-determining step are found for enones **5** and **6**. Reversibility is expected to have a significant effect on the net reactivity for these enones.

■ CONCLUSIONS

CBS-QB3 calculations in conjunction with the CPCM solvent model indicate that the activation energies for conjugate additions of MeSH to α,β-unsaturated ketones in water are raised by 2−6 kcal mol^{-1} when α-Me, β-Me, β,β-dimethyl, or β-Ph substitution is present on the C=C bond. The free energy of the overall transformation is raised by 4−8 kcal mol^{-1}. Accumulation of protobranches does not stabilize a more highly substituted adduct sufficiently to make up for the loss of hyperconjugative stabilization from the reactant (as has previously

BeiGene Exhibit 1157.006
BeiGene v. Pharmacyclics
PGR2024-00009

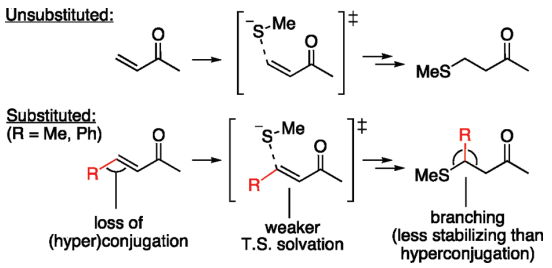

Figure 5. Summary of the interactions responsible for the lower reactivities of substituted α,β-unsaturated ketones toward conjugate additions of thiols.

been found for C−C and C−O bond-forming reactions).[14,36] Weaker solvation of the more highly substituted transition states magnifies the alkyl-group effects on the activation energies. The kinetics and thermodynamics of thiol additions are predicted with only low accuracy by common DFT and ab initio methods, but the more recently developed M06-2X (with a good basis set), B2PLYP-D, and SCS-MP2 do provide reliable energetics. These factors are summarized in Figure 5.

■ ASSOCIATED CONTENT

Supporting Information. Molecular coordinates and energies, and complete citations for refs 4, 6, 33, and 34. This material is available free of charge via the Internet at http://pubs.acs.org.

■ AUTHOR INFORMATION

Corresponding Author
*E-mail: ekrenske@unimelb.edu.au, houk@chem.ucla.edu

■ ACKNOWLEDGMENT

We thank the National Science Foundation and Australian Research Council for generous financial support (CHE-0548209 to K.N.H. and DP0985623 to E.H.K.), and the NCSA, UCLA ATS, UCLA IDRE, and NCF NI (Australia) for computer resources.

■ REFERENCES

(1) Metal-ion and Brønsted acid catalysis of these reactions are also known. For examples and asymmetric applications of conjugate additions of thiols to α,β-unsaturated ketones, see: (a) Trost, B. M.; Keeley, D. E. *J. Org. Chem.* **1975**, *40*, 2013. (b) Dinon, F.; Richards, E.; Murphy, P. J.; Hibbs, D. E.; Hursthouse, M. B.; Abdul Malik, K. M. *Tetrahedron Lett.* **1999**, *40*, 3279–3282. (c) Sibi, M. P.; Manyem, S. *Tetrahedron* **2000**, *56*, 8033–8061. (d) McDaid, P.; Chen, Y.; Deng, L. *Angew. Chem., Int. Ed.* **2002**, *41*, 338–340. (e) Kamimura, A.; Morita, R.; Matsuura, K.; Omata, Y.; Shirai, M. *Tetrahedron Lett.* **2002**, *43*, 6189–6191. (f) Kamimura, A.; Morita, R.; Matsuura, K.; Mitsudera, H.; Shirai, M. *Tetrahedron* **2003**, *59*, 9931–9938. (g) Garg, S. K.; Kumar, R.; Chakraborti, A. K. *Synlett* **2005**, 1370–1374. (h) Garg, S. K.; Kumar, R.; Chakraborti, A. K. *Tetrahedron Lett.* **2005**, *46*, 1721–1724. (i) Kataoka, T.; Kinoshita, H. *Phosphorus, Sulfur, and Silicon* **2005**, *180*, 989–992. (j) Rao, J. S.; Brière, J.-F.; Metzner, P.; Basavaiah, D. *Tetrahedron Lett.* **2006**, *47*, 3553–3556. (k) Kamimura, A.; Okawa, H.; Morisaki, Y.; Ishikawa, S.; Uno, H. *J. Org. Chem.* **2007**, *72*, 3569–3572. (l) Sharma, G.; Kumar, R.; Chakraborti, A. K. *Tetrahedron Lett.* **2008**, *49*, 4272–4275.

(2) E.g. (a) Powers, J. C.; Asgian, J. L.; Ekici, Ö. D.; James, K. E. *Chem. Rev.* **2002**, *102*, 4639–4750. (b) Vicik, R.; Busemann, M.; Baumann, K.; Schirmeister, T. *Curr. Top. Med. Chem.* **2006**, *6*, 331–353. (c) Groll, M.; Schellenberg, B.; Bachmann, A. S.; Archer, C. R.; Huber, R.; Powell, T. K.; Lindow, S.; Kaiser, M.; Dudler, R. *Nature* **2008**, *452*, 755–759. (d) Baldisserotto, A.; Destro, F.; Vertuani, G.; Marastoni, M.; Gavioli, R.; Tomatis, R. *Bioorg. Med. Chem.* **2009**, *17*, 5535–5540. (e) Recent reviews of covalent drugs are given in: Singh, J.; Petter, R. C.; Baillie, T. A.; Whitty, A. *Nature Rev. Drug Discovery* **2011**, *10*, 307−317. Singh, J.; Petter, R. C.; Kluge, A. F. *Curr. Opin. Chem. Biol.* **2010**, *14*, 475−480.

(3) Zhang, J.; Yang, P. L.; Gray, N. S. *Nature Rev. Canc.* **2009**, *9*, 28–39.

(4) Wong, K.-K.; et al. *Clin. Cancer Res.* **2009**, *15*, 2552–2558 and references cited therein.

(5) Eskens, F. A. L. M.; Mom, C. H.; Planting, A. S. T.; Gietema, J. A.; Amelsberg, A.; Huisman, H.; van Doorn, L.; Burger, H.; Stopfer, P.; Verweij, J.; de Vries, E. G. E. *Brit. J. Canc.* **2008**, *98*, 80–85 and references cited therein.

(6) Pan, Z.; et al. *ChemMedChem* **2007**, *2*, 58–61.

(7) (a) Dmuchovsky, B.; Vineyard, B. D.; Zienty, F. B. *J. Am. Chem. Soc.* **1964**, *86*, 2874–2877. (b) Friedman, M.; Cavins, J. F.; Wall, J. S. *J. Am. Chem. Soc.* **1965**, *87*, 3672–3682. (c) De Maria, P.; Fini, A. *J. Chem. Soc. (B)* **1971**, 2335–2338. (d) Semenow-Garwood, D. *J. Org. Chem.* **1972**, *37*, 3797–3803. (e) Bickley, J. F.; Ciucci, A.; Evans, P.; Roberts, S. M.; Ross, N.; Santoro, M. G. *Bioorg. Med. Chem.* **2004**, *12*, 3221–3227. (f) Khatik, G. L.; Kumar, R.; Chakraborti, A. K. *Org. Lett.* **2006**, *8*, 2433–2436. (g) Hartman, R. F.; Rose, S. D. *J. Org. Chem.* **2006**, *71*, 6342–6350.

(8) For a discussion of substituent effects on the related conjugate hydrocyanations of acrylates and acrylonitriles: Nagata, W.; Yoshioka, M. *Organic Reactions* **1977**, *25*, 255–476. α-Methyl, β-methyl, β,β-dimethyl, and β-phenyl substitution impede hydrocyanation, while α-phenyl substitution accelerates hydrocyanation. Substituent effects on conjugate additions of organometallic nucleophiles to α,β-unsaturated ketones are reviewed in: Duval, D.; Géribaldi, S. In *The Chemistry of Enones*; Patai, S., Rappoport, Z., Eds.; Wiley: Chichester, 1989; pp 355−469.

(9) (a) Esterbauer, H.; Zollner, H.; Scholz, N. *Z. Naturforsch., C* **1975**, *30c*, 466–473. (b) Chan, J. W.; Hoyle, C. E.; Lowe, A. B.; Bowman, M. *Macromolecules* **2010**, *43*, 6381–6388. (c) Schwöbel, J. A. H.; Wondrousch, D.; Koleva, Y. K.; Madden, J. C.; Cronin, M. T. D.; Schüürmann, G. *Chem. Res. Toxicol.* **2010**, *23*, 1576–1585. (d) Böhme, A.; Thaens, D.; Schramm, F.; Paschke, A.; Schüürmann, G. *Chem. Res. Toxicol.* **2010**, *23*, 1905–1912.

(10) (a) van Axel Castelli, V.; Bernardi, F.; Dalla Cort, A.; Mandolini, L.; Rossi, I.; Schiaffino, L. *J. Org. Chem.* **1999**, *64*, 8122–8126. (b) van Axel Castelli, V.; Dalla Cort, A.; Mandolini, L.; Reinhoudt, D. N.; Schiaffino, L. *Eur. J. Org. Chem.* **2003**, 627–633.

(11) (a) Karabunarliev, S.; Mekenyan, O. G.; Karcher, W.; Russom, C. L.; Bradbury, S. P. *Quant. Struct.-Act. Relat.* **1996**, *15*, 302–310. (b) Steert, K.; El-Sayed, I.; Van der Veken, P.; Krishtal, A.; Van Alsenoy, C.; Westrop, G. D.; Mottram, J. C.; Coombs, G. H.; Augustyns, K.; Haemers, A. *Bioorg. Med. Chem. Lett.* **2007**, *17*, 6563–6566. (c) Oballa, R. M.; Truchon, J.-F.; Bayly, C. I.; Chauret, N.; Day, S.; Crane, S.; Berthelette, C. *Bioorg. Med. Chem. Lett.* **2007**, *17*, 998–1002. (d) Cronin, M. T. D.; Bajot, F.; Enoch, S. J.; Madden, J. C.; Roberts, D. W.; Schwöbel, J. *ATLA, Altern. Lab. Anim.* **2009**, *37*, 513–521. (e) Wondrousch, D.; Böhme, A.; Thaens, D.; Ost, N.; Schüürmann, G. *J. Phys. Chem. Lett.* **2010**, *1*, 1605–1610.

(12) Schwöbel, J. A. H.; Madden, J. C.; Cronin, M. T. D. *SAR QSAR Environ. Res.* **2010**, *21*, 693–710.

(13) (a) Montgomery, J. A., Jr.; Frisch, M. J.; Ochterski, J. W.; Petersson, G. A. *J. Chem. Phys.* **1999**, *110*, 2822–2827. (b) Montgomery, J. A., Jr.; Frisch, M. J.; Ochterski, J. W.; Petersson, G. A. *J. Chem. Phys.* **2000**, *112*, 6532–6542.

(14) Wheeler, S. E.; Moran, A.; Pieniazek, S. N.; Houk, K. N. *J. Phys. Chem. A* **2009**, *113*, 10376–10384.

BeiGene Exhibit 1157.007
BeiGene v. Pharmacyclics
PGR2024-00009

(15) Pieniazek, S. N.; Clemente, F. R.; Houk, K. N. *Angew. Chem., Int. Ed.* **2008**, *47*, 7746–7749.
(16) Curtiss, L. A.; Raghavachari, K.; Redfern, P. C.; Rassolov, V.; Pople, J. A. *J. Chem. Phys.* **1998**, *109*, 7764–7776.
(17) (a) Guner, V.; Khuong, K. S.; Leach, A. G.; Lee, P. S.; Bartberger, M. D.; Houk, K. N. *J. Phys. Chem. A* **2003**, *107*, 11445–11459. (b) Ess, D. H.; Houk, K. N. *J. Phys. Chem. A* **2005**, *109*, 9542–9553.
(18) Zheng, J.; Zhao, Y.; Truhlar, D. G. *J. Chem. Theory Comput.* **2007**, *3*, 569–582.
(19) (a) Lee, C.; Yang, W.; Parr, R. G. *Phys. Rev. B* **1988**, *37*, 785–789. (b) Becke, A. D. *J. Chem. Phys.* **1993**, *98*, 1372–1377. (c) Becke, A. D. *J. Chem. Phys.* **1993**, *98*, 5648–5652.
(20) (a) Burke, K.; Perdew, J. P.; Wang, Y. In *Electronic Density Functional Theory: Recent Progress and New Directions*; Dobson, J. F., Vignale, G., Das, M. P., Eds.; Plenum: New York, 1988. (b) Perdew, J. P. In *Electronic Structure of Solids '91*; Ziesche, P., Eschrig, H., Eds.; Akademie: Berlin, 1991; p 11. (c) Perdew, J. P.; Chevary, J. A.; Vosko, S. H.; Jackson, K. A.; Pederson, M. R.; Singh, D. J.; Fiolhais, C. *Phys Rev. B* **1992**, *46*, 6671–6687; *48*, 4978. (d) Perdew, J. P.; Burke, K.; Wang, Y. *Phys. Rev. B* **1996**, *54*, 16533–16539. (e) Adamo, C.; Barone, V. *J. Chem. Phys.* **1998**, *108*, 664–675.
(21) Becke, A. D. *J. Chem. Phys.* **1996**, *104*, 1040–1046.
(22) (a) Perdew, J. P.; Burke, K.; Ernzerhof, M. *Phys. Rev. Lett.* **1996**, *77*, 3865–3868. *78*, 1396. (b) Adamo, C.; Barone, V. *J. Chem. Phys.* **1999**, *110*, 6158–6170.
(23) Zhao, Y.; Truhlar, D. G. *Theor. Chem. Acc.* **2008**, *120*, 215–241.
(24) Grimme, S. *J. Chem. Phys.* **2006**, *124*, 034108−1–034108−16.
(25) Schwabe, T.; Grimme, S. *Phys. Chem. Chem. Phys.* **2007**, *9*, 3397–3406.
(26) Binkley, J. S.; Pople, J. A. *Int. J. Quantum Chem.* **1975**, *9*, 229–236.
(27) (a) Grimme, S. *J. Chem. Phys.* **2003**, *118*, 9095–9102. (b) Gerenkamp, M.; Grimme, S. *Chem. Phys. Lett.* **2004**, *392*, 229–235. (c) Grimme, S. *J. Phys. Chem. A* **2005**, *109*, 3067–3077.
(28) SCS-MP2 calculations were performed on the MP2-optimized geometries.
(29) (a) Liljefors, T.; Allinger, N. L. *J. Am. Chem. Soc.* **1976**, *98*, 2745–2749. (b) Naito, I.; Kinoshita, A.; Yonemitsu, T. *Bull. Chem. Soc. Jpn.* **1976**, *49*, 339–340. (c) Liljefors, T.; Allinger, N. L. *J. Am. Chem. Soc.* **1978**, *100*, 1068–1073. (d) García, J. I.; Mayoral, J. A.; Salvatella, L.; Assfeld, X.; Ruiz-López, M. F. *J. Mol. Struct.: THEOCHEM* **1996**, *362*, 187–197. (e) Bokareva, O. S.; Bataev, V. A.; Godunov, I. A. *J. Mol. Struct: THEOCHEM* **2009**, *913*, 254–264.
(30) (a) Barone, V.; Cossi, M. *J. Phys. Chem. A* **1998**, *102*, 1995–2001. (b) Barone, V.; Cossi, M.; Tomasi, J. *J. Comput. Chem.* **1998**, *19*, 404–417.
(31) (a) Vayner, G.; Houk, K. N.; Jorgensen, W. L.; Brauman, J. I. *J. Am. Chem. Soc.* **2004**, *126*, 9054–9058. (b) Chen, X.; Regan, C. K.; Craig, S. L.; Krenske, E. H.; Houk, K. N.; Jorgensen, W. L.; Brauman, J. I. *J. Am. Chem. Soc.* **2009**, *131*, 16162–16170.
(32) (a) Gonzalez, C.; Schlegel, H. B. *J. Chem. Phys.* **1989**, *90*, 2154–2161. (b) Gonzalez, C.; Schlegel, H. B. *J. Phys. Chem.* **1990**, *94*, 5523–5527.
(33) Frisch, M. J.; et al. *Gaussian 03*, Revision C.02; Gaussian, Inc., Wallingford CT, 2004.
(34) Frisch, M. J.; et al. *Gaussian 09*, Revision A.02; Gaussian, Inc., Wallingford CT, 2009.
(35) Legault, C. Y. CYLview, 1.0b; Université de Sherbrooke, 2009 (http://www.cylview.org).
(36) (a) Grimme, S. *Angew. Chem., Int. Ed.* **2006**, *45*, 4460–4464. (b) Wodrich, M. D.; Corminboeuf, C.; Schleyer, P. v. R. *Org. Lett.* **2006**, *8*, 3631–3634. (c) Wodrich, M. D.; Wannere, C. S.; Mo, Y.; JarowskiP. D.; Houk, K. N.; Schleyer, P. v. R. *Chem.—Eur. J.* **2007**, *13*, 7731–7744. (d) Wodrich, M. D.; Jana, D. F.; Schleyer, P. v. R.; Corminboeuf, C. *J. Phys. Chem. A* **2008**, *112*, 11495–11500. (e) Schleyer, P. v. R.; McKee, W. C. *J. Phys. Chem. A* **2010**, *114*, 3737–3740.
(37) Protobranching is defined in ref 36c as "the net stabilizing 1,3-alkyl−alkyl interactions present in linear, branched, and most cycloalkanes, but not in methane or ethane".
(38) Kunakbaeva, Z.; Carrasco, R.; Rozas, I. *J. Mol. Struct.: THEOCHEM* **2003**, *626*, 209–216.
(39) Calculations at the B3LYP/6-31+G(d) level reported in Mohamed, A. A.; Jensen, F. *J. Phys. Chem. A* **2001**, *105*, 3259–3268.
(40) The LUMO of **6** is 0.9 eV lower than that of **1**. Orbitals calculated at the HF/6-31G//B3LYP/CBSB7 level.

BeiGene Exhibit 1157.008
BeiGene v. Pharmacyclics
PGR2024-00009